IEEE Access
Multidisciplinary | Rapid Review | Open Access Journal

Received June 11, 2019, accepted July 7, 2019, date of publication July 16, 2019, date of current version August 7, 2019.

Digital Object Identifier 10.1109/ACCESS.2019.2929273

A Vehicle Mobile Internet of Things Coverage Enhancement Algorithm Based on Communication Duration Probability Analysis

ZHIPING WAN[1], ZHIHONG PAN[1], WEICHUAN NI[2], FENG WANG[1], ZEMIN QIU[1], SHAOJIANG LIU[2], AND ZHIMING XU[1]

[1]Department of Information Science, Xinhua College of Sun Yat-sen University, Guangzhou 510520, China
[2]Department of Equipment and Laboratory Management, Xinhua College of Sun Yat-sen University, Guangzhou 510520, China

Corresponding author: Zhiping Wan (wzp888@xhsysu.edu.cn)

ABSTRACT Vehicle mobile Internet of Things uses sensor technology, mobile Internet technology, and intelligent computing technology to effectively monitor and provide comprehensive services for vehicle operation status. It is an important part of building a smart city, making urban transportation more efficient, environmentally friendly, intelligent, and safety. In the vehicle mobile Internet of Things, when in-vehicle sensors are in communication with each other, they are often affected by factors, such as network mobility, transmission range, and signal interference. Therefore, in order to ensure the continuity of communication between nodes and improve the quality of network communication, this paper proposes a vehicle mobile Internet of Things coverage enhancement algorithm (PANM). First, we derive the probabilistic analysis model of communication duration by analyzing the functional relationship of vehicle initial velocity, acceleration, spacing distance, and communication duration. Then, under the premise of ensuring the communication duration, in order to improve the coverage of the vehicle mobile Internet of Things, the network overlap ratio is introduced in the probability analysis model. Finally, we improve the network coverage performance of omnidirectional radiation and fan-shaped radiation communication models of vehicle mobile Internet of Things by limiting the overlap ratio threshold. The experimental simulation results indicate that the PANM algorithm can reduce the packet loss rate of the vehicle network and have a shorter communication delay.

INDEX TERMS Vehicle mobile Internet of Things, communication duration, probability analysis, overlap ratio, network coverage enhancement algorithm.

I. INTRODUCTION

Cyber Physics System (CPS) is a multi-dimensional complex system integrating computing, network and physical environment. Vehicle mobile internet of things as one of the main research fields of CPS, has received the attention of many researchers in recent years. VMIT (Vehicle Mobile Internet of Things) is an overlay network established by a vehicle equipped with a remote communication device or a communication device with a certain sensing range [1], [2]. The VMIT can collect the data of the location of the vehicle and its surroundings and transmit the data to other vehicles, remote base stations and satellite terminals in the network coverage area through multi-hop forwarding or transmitting terminals [3], [4]. With the effective combination of automatic control technology, artificial intelligence, information technology, communication technology, and transportation system, as well as the development of vehicle driverless technology, making it possible to build an urbanized transportation system with intelligent control, efficient operation, orderly management, precise positioning and safe driving [5], [6]. Among them, the short-range vehicle mobile internet of things technology based on location information has been put into use, the U.S. Federal Communications Commission (FCC) allocated a 75 MHz spectrum to the vehicle network in the 5.9 GHz ISM (Industrial, Scientific,

The associate editor coordinating the review of this manuscript and approving it for publication was Chunsheng Zhu.

and Medical) band [7], [8], and DSRCs (Dedicated Short Range Communications) limit the wireless communication between vehicles within about 300m.

Many scholars already have certain scientific research achievements in the communication problem of vehicle mobile internet of things. Kumar *et al.* [9] proposed an agent learning–based clustering algorithm in vehicle mobile internet of things (ALCA). They take into account the high mobility of the vehicle mobile internet of things nodes, making it difficult for cluster heads to maintain normal communication with mobile nodes within their communication range. Therefore, this algorithm uses the base station deployed on the roadside as the agent unit to coordinate the inter-area vehicle intercommunication through the density and average speed information of the vehicle. Compared with the direct communication between vehicles, the ALCA algorithm is less affected by vehicle mobility, but deploying multiple base stations along the road requires a greater economic cost. Ucar *et al.* [10] proposed a vehicular multi-hop algorithm for stable clustering (VMaSC) for VMIT. The algorithm considers the relative mobility of vehicles and the average relative velocity between adjacent vehicles in the same direction and adopts multi-hop clustering method to increase the communication duration between cluster heads and cluster members. But the VMaSC ignores the analysis of the speed state and distance relationship between vehicles[11]–[13].

However, the research work for enhancing coverage area of the vehicle network under the condition of guaranteeing the normal communication of vehicle internet of things area, which is still very rare. And with the continuous development of intelligent transportation system, the application demand of vehicle network is indispensable [14], [15]. How to increase the network coverage to expand the scope of data collection and reduce the overlapping area to save network energy will become an important issue for vehicle network research[16]–[18]. As the more mature land-based wireless sensor network technology, the problem of network coverage enhancement has also become an important aspect of the study of terrestrial wireless sensor networks [19], [20].

In this paper, according to the communication distance limit under the DSRCs standard in the actual application scenario, we obtain a function of the vehicle communication duration by analyzing the vehicle speed relationship within the communication critical distance. In order to improve the robustness, this function includes the relationship between the distance and the duration of the vehicle in the variable speed state. When the communication between the vehicles needs to satisfy a certain time, the current distance between vehicles can be adjusted according to the function to ensure that the communication link will not be interrupted. In order to increase the coverage rate of vehicle mobile internet of things, we introduce the concept of vehicle network coverage overlap ratio and analyze the coverage overlap ratio of vehicle mobile internet of things under omnidirectional radiation and fan-shaped radiation communication models respectively. We derive the distance between the vehicles and the orientation angle of the sensors at the minimum overlap ratio of the two communication models and give a proof of this.

The second section introduces the vehicle IoT network communication model, mainly introduces two kinds of on-board sensor radiation models, namely omnidirectional radiation and fan-shaped radiation models. The third section introduces the PANM algorithm, which proposes a communication duration function equation to analyzes the moving speed and acceleration of the communication vehicle without interruption of the communication link, and proposes the network coverage enhancement method under the omnidirectional radiation model and the fan radiation model is proposed. Section 4 conducted experimental simulations and data analysis.

II. VEHICLE NETWORK COMMUNICATION MODEL

It is assumed that vehicles on the traffic lane need to communicate with each other, to obtain relevant data information of the other vehicle. Figure 1 shows a vehicle model with randomly distributed vehicles when the radiation methods of the vehicular sensor is an omnidirectional radiation. And figure 2 shows a vehicle model with randomly distributed vehicles when the radiation method of the vehicular sensor is a fan-shaped radiation. In both models, R represents the sensor's sensing radius, and L represents the spacing distance between two vehicles. Assuming that the vehicle network communication in the model adopts the DSRCs standard, the maximum communication distance is 300m. When the distance between vehicles exceeds 300m, the communication link is immediately interrupted [21], [22]. In the model, the shaded area indicates the overlap area between the sensor sensing range of the vehicle.

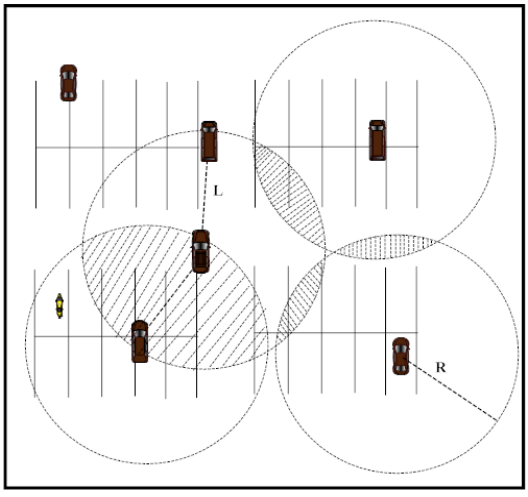

FIGURE 1. The communication model that radiation methods is omnidirectional radiation.

The link distance between vehicles is$L = \sum_{i=0}^{n} L_i$, that is, the distance between the source vehicle and the target vehicle in communication. $\sum_{i=0}^{n} L_i$ indicates that the link distance L

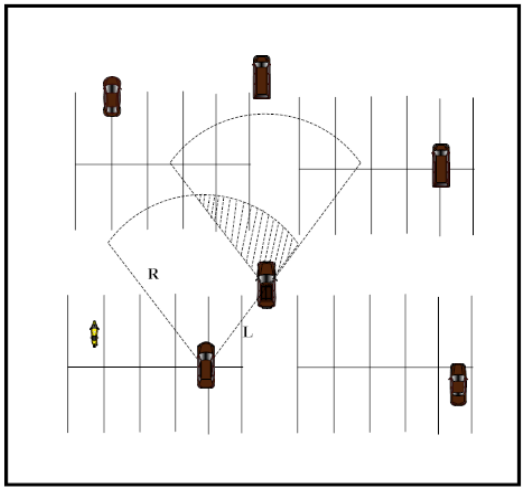

FIGURE 2. The communication model that radiation methods is Fan-shaped.

is divided into n intervals between the source vehicle and the target vehicle.

L_i is a random variable with a logarithmic normal distribution, thus $L_i \in \log N(\mu_i, \sigma_i)$, and the probability density function of the lognormal distribution is [23]:

$$f(L_i; \mu_i, \sigma_i) = \frac{1}{x\sigma_i\sqrt{2\pi}} e^{-(\ln x-\mu_i)^2/2\sigma_i^2} \tag{1}$$

The expected value $E(x)$ and the variance $V(x)$ are respectively:

$$\begin{cases} E(L_i) = e^{\mu_i+\sigma_i^2/2} \\ V(L_i) = \left(e^{\sigma_i^2}-1\right) e^{2\mu_i+\sigma_i^2} \end{cases} \tag{2}$$

L is approximately obey log normal [24], $L \in \log N(\mu_L, \sigma_L)$, we can get:

$$\begin{cases} \mu_L = \ln(E(L_i)) - \frac{1}{2}\ln\left(1+\frac{V(L_i)}{E(L_i)^2}\right) \\ \sigma_L^2 = \ln\left(1+\frac{V(L_i)}{E(L_i)^2}\right) \end{cases} \tag{3}$$

Link loss is represented by $Loss(L)$. As vehicular sensor uses wireless communication technology, when eliminating external interference, the attenuation of signal mainly considers the influence of link distance [25]:

$$Loss(L) = 40\log L - 10(\log G_l + \log G_r) - 20(\log h_l + \log h_r) \tag{4}$$

where G_l is transmitter antenna gain, G_r is receiver antenna gain, h_l is transmitter antenna height, h_r is receiver antenna height. We assume that the maximum loss threshold that the link can tolerate in the communication model is TL, and the probability distribution function of the link loss allowed in the communication is:

$$P(Loss(L) \le TL) = \int_{-\infty}^{TL} \frac{1}{40} \cdot \frac{1}{\sigma_{TL}\sqrt{2\pi}} \cdot e^{\left(-\frac{(x-\mu_{TL})^2}{2\sigma_{TL}^2}\right)} dx \tag{5}$$

III. PANM ALGORITHMS

A. COMMUNICATION DURATION FUNCTION

Since the DSRCs standard communication distance is limited to 300m, the 300m vehicle spacing distance is the critical point for communication link disruption [26], [27]. Let the initial interval between the source vehicle and the target vehicle be L_0 ($0 < L_0 < 300m$). When the communication distance is not yet near the critical point, the vehicle is uniformly accelerated or uniformly decelerated, the initial speed of the source vehicle is v_0 and the acceleration is a_0. The initial speed of the target vehicle is v_0' and the acceleration is a_0. The function representation of communication duration is:

$$\begin{cases} L_0 - S_i(t) + S_j(t) = L \\ S_i(t) = \int_0^t (v_0 + a_0 x)dx \\ S_j(t) = \int_0^t (v_0' + a_0' x)dx \end{cases} \tag{6}$$

Assuming that the required communication duration between vehicles is t_1, the spacing distance L in this communication needs to satisfy $-300 \le L \le 300$, that is, whether the time t when converting the problem to $L = -300$ or $L = 300$ satisfies $t \ge t_1$ or not, the function representation of communication duration when $L = 300$ is

$$L_0 - S_i(t) + S_j(t) = 300 \tag{7}$$

In order to satisfy the expression (7), the initial velocity and acceleration between the source vehicle and the target vehicle have the following relations:

$$\begin{cases} v_0 \le v_0' & a_0 < a_0' \\ v_0 < v_0' & a_0 > a_0' \\ v_0 > v_0' & 0 \le a_0 < a_0' \\ v_0 > v_0' & a_0 < 0 \le a_0' \end{cases} \tag{8}$$

And the corresponding time t is satisfied

$$\begin{cases} t = \frac{(v_0-v_0')+\sqrt{(v_0'-v_0)^2+2(a_0'-a_0)(300-L_0)}}{(a_0'-a_0)} \\ t = \frac{v_0'-v_0}{a_0-a_0'} \\ t = \frac{(v_0-v_0')+\sqrt{(v_0'-v_0)^2+2(a_0'-a_0)(300-L_0)}}{(a_0'-a_0)} \\ t = \frac{(v_0-v_0')+\sqrt{(v_0'-v_0)^2+2(a_0'-a_0)(300-L_0)}}{(a_0'-a_0)} \end{cases} \tag{9}$$

When $L = -300$, the function of communication duration is expressed as

$$L_0 - S_i(t) + S_j(t) = -30 \tag{10}$$

In order to satisfy the expression (10), the initial velocity and acceleration between the source vehicle and the target vehicle have the following relations:

$$\begin{cases} v_0 \ge v_0' & a_0 > a_0' \\ v_0 < v_0' & a_0 > a_0' \ge 0 \\ v_0 < v_0' & a_0 \ge 0 > a_0' \\ v_0 > v_0' & 0 \le a_0 < a_0' \\ v_0 > v_0' & a_0 < 0 \le a_0' \end{cases} \tag{11}$$

And the corresponding time t is satisfied:

$$\begin{cases} t = \frac{(v_0'-v_0)+\sqrt{(v_0-v_0')^2+2(a_0-a_0')(300+L_0)}}{(a_0-a_0')} \\ t = \frac{(v_0'-v_0)+\sqrt{(v_0-v_0')^2+2(a_0-a_0')(300+L_0)}}{(a_0-a_0')} \\ t = \frac{(v_0'-v_0)+\sqrt{(v_0-v_0')^2+2(a_0-a_0')(300+L_0)}}{(a_0-a_0')} \\ t = \frac{v_0-v_0'}{a_0'-a_0} \\ t = \frac{v_0-v_0'}{a_0'-a_0} \end{cases} \tag{12}$$

Lemma 1: The communication duration t can be expressed as the square root function of L_0.

Proof: The source vehicle's driving distance function is:

$$S_i(t) = \int_0^t (v_0 + a_0 x)dx = v_0 t + \frac{1}{2}a_0 t^2 \tag{13}$$

The target vehicle's driving distance function is:

$$S_j(t) = \int_0^t (v_0' + a_0' x)dx = v_0' t + \frac{1}{2}a_0' t^2 \tag{14}$$

We can get the quadratic equation:

$$S_j(t) - S_i(t) = (v_0' - v_0)t + \frac{1}{2}(a_0' - a_0)t^2 = L - L_0 \tag{15}$$

Therefore, the solution of t is converted into the square root function of L_0, which can be proved.

Lemma 2: $a+\sqrt{b+cL_0}$ submits to lognormal distribution.

Proof: Find the probability distribution function of $(a + \sqrt{b + cL_0}) \leq N$:

$$P(a + \sqrt{b + cL_0} \leq N) = P(\frac{(N-a)^2 - b}{c} \geq L_0 \tag{16}$$

Given that L_i is a random variable with log-normal distribution, therefore $a + \sqrt{b + cL_0}$ obeys a lognormal distribution.

Lemma 3: Communication duration t submits to lognormal distribution.

Proof: Lemma 1 can prove that t can be expressed as the square root function of L_0, Lemma 2 can prove that the square root function of L_0 submits to the lognormal distribution, so Lemma 3 holds.

The maximum communication duration t can be obtained from the initial velocity, acceleration, initial spacing distance and the maximum separation distance of the source vehicle and the target vehicle. And the size relationship between t_1 and t is judged according to the required communication duration t_1 between vehicles. When $t_1 > t$, the strategy of adjusting the acceleration is adopted to increase t to satisfy $t_1 \leq t$, thus ensuring that the link will not be interrupted during communication.

B. NETWORK COVERAGE ENHANCEMENT

It is known that the required communication duration between the source vehicle and the target vehicle is t_1 and the sensing radius of the sensor is $R(R > 300)$. The overlapping ratio within the sensing range of the vehicular sensor is indicated by η, that is, the ratio of the overlap area between the source vehicle and the target vehicle to the total area covered. In the model at Figure 3, the closer the communication interval between vehicles is, the greater the overlap ratio is, and conversely, the longer the communication distance, the smaller the overlap ratio is. But it needs to ensure that the communication distance cannot exceed 300m. In the model of Figure 4, the overlap ratio is reduced by properly adjusting the orientation of the vehicle sensor without breaking the communication link.

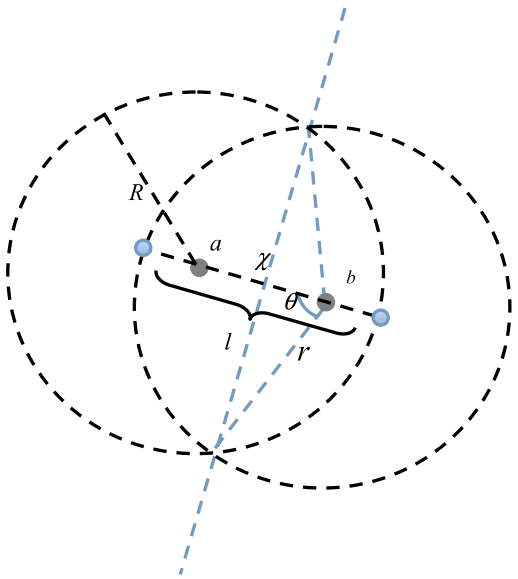

FIGURE 3. Overlap ratio analysis model of omnidirectional radiation pattern.

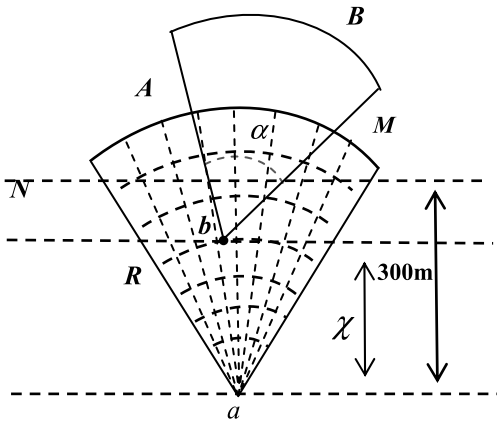

FIGURE 4. Overlap ratio analysis model of Fan-shaped radiation pattern.

1) OMNIDIRECTIONAL RADIATION COMMUNICATION MODEL

Figure 3 is a model for the specific analysis of overlay of vehicular sensor on the basis of Figure 1. Where a is source vehicle, b is target vehicle, the spacing distance between a and b is represented by χ, the overlapping area of the a and b radiation ranges is the coverage overlap area of the current network. Let l be the coverage length, which represents the

spacing distance between the two points that are the furthest apart in the overlapping area, and they are located on the straight lines between $a$and$b$. Assuming that the overlapping area between a and b is S_{ab}, the calculation method of S_{ab} can be converted to the method of calculating fan-shaped area minus the area of triangle by means of average segmentation. As shown in Figure 3, when the fan-shaped radius is r, the area of S_{ab} can be obtained:

$$S_{ab} = 2 \cdot (\frac{2\theta\pi r^2}{360^0} - \frac{1}{2} \cdot 2 \cdot \sin\theta \cdot r \cdot \cos\theta \cdot r) \quad (17)$$

The overlapping ratio $\eta = \frac{S_{ab}}{\pi R^2}$ can be obtained. The relationship between the radius r and the radius θ of the fan-shaped is $r = \frac{1}{2}l + r \cdot \cos\theta$, and the relationship between the covering length l and the spacing distance χ between a and b is $l = 2R - \chi$. That is:

$$r = \frac{2R - \chi}{2(1 - \cos\theta)} \quad (18)$$

Since the distance χ between a and b satisfies $0 < \chi < R$, so for a fan-shaped, θ can be obtained as $\cos\theta = \frac{\chi}{2R}$. Substituting $\cos\theta = \frac{\chi}{2R}$ and Eq. (18) into Eq. (17), the relation between the overlap ratio η and the spacing distance χ can be obtained as:

$$\chi = 2R\left[1 - (1 - \frac{\chi}{2R}) \cdot \sqrt{\frac{\eta\pi}{2 \cdot (\frac{2\arccos\theta \cdot \pi}{360^0} - \sqrt{1 - \frac{\chi^2}{4R^2}} \cdot \frac{\chi}{2R})}}\right] \quad (19)$$

When communication between a and b continues until a certain time $t(t \leq t_1)$, by substituting Eq. (19) into Eq. (20):

$$S_b(t) - S_a(t) = (v_b - v_a)t + \frac{1}{2}(a_b - a_a)t^2 = \chi \quad (20)$$

The overlap ratio at a certain time t can be obtained.

As can be seen from the Eq. (19), when the communication link is not interrupted, the greater the spacing distance χ between a and b, the smaller the overlap ratio η is. Set an overlap ratio threshold $\eta_{\text{Threshold}}$, the overlap rate threshold is determined by the user. When $\eta > \eta_{\text{Threshold}}$, proper adjustment of the spacing distance between vehicles, so that η is less than $\eta_{\text{Threshold}}$. Since the maximum spacing distance between a and b is $\chi = 300$m, when the spacing distance between a and b always stays at 300m, the overlap ratio η remains the minimum during communication. When the distance between the two vehicles is greater than the sensor sensing radius χ, although the overlap ratio is smaller, the communication link between the two vehicles will be disconnected.

2) FAN-SHAPED RADIATION COMMUNICATION MODEL

Figure 4 is a model for the specific analysis of the overlap ratio of the vehicle network in a fan-shaped radiation pattern. The sensors on the source vehicle and the target vehicle are expressed in points a and b respectively, and the spacing distance between a and b is expressed by χ. The radiation range angle of the vehicular sensor is α, and the coverage area of a and b are respectively represented by A and B (both are equal in area). Due to the irregularities in the overlapping regions A and B, the method of covering grid is used here to calculate the coverage area, as shown in Figure 4, N and M denote grids with N rows and M columns, respectively. That is, the coverage area of a is divided into $N \times M$ grids. We can get the overlapped area of A and B by calculating the area of each grid covered by the overlap area. Let a grid (k, q) of a $k(k \leq N)$ row and $q(q \leq M)$ column be in the overlapping area, and the area of the grid can be obtained as follows:

$$S_{kq} = \frac{1}{2} \cdot \frac{\alpha}{M} \cdot (\frac{R}{N} \cdot k)^2 - \frac{1}{2} \cdot \frac{\alpha}{M} \cdot (\frac{R}{N} \cdot (k-1))^2 \quad (21)$$

Let S_{ab} be the sum of the areas of all the grids in the coverage area, then $\eta = \frac{2S_{ab}}{\alpha R^2}$. Some grids are only part of their own area in the coverage area, but in calculating the area of these grids is to calculate the total area. So there is a certain error between S_{ab} and the actual overlap area. For this problem, we can reduce the error by increasing the number of $N \times M$ grids in the calculation.

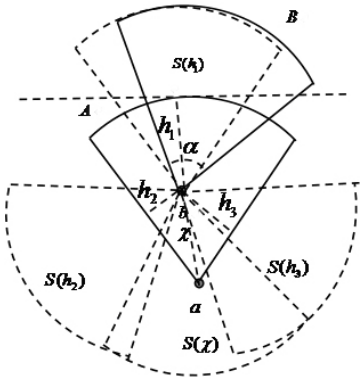

(a) The overlapping area of the different radiation direction.

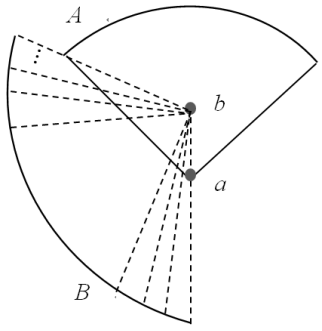

(b) The minimum overlapping area

FIGURE 5. Cover overlapping area analysis model.

When the calculated overlap ratio η appears in the case of $\eta > \eta_{\text{Threshold}}$, in addition to the measures taken to increase the spacing distance χ without any interruption of the link, the coverage overlap area can be reduced more effectively by adjusting the radiation direction of the vehicular sensor b. Taking the vehicular sensor b in Figure 5 (a) as an example, at this point $\eta > \eta_{\text{Threshold}}$, calculate the arc length of b to the

fan-shaded area A, the radius of both ends and the shortest distance of point a, as the straight lines h_1, h_2, h_3 and the spacing distance χ, respectively. The shortest distance to the arc length is the Euclidean distance between these two points when the straight line starting from point b is perpendicular to the tangent of a point on the arc. We assume that when the radiation range angle α of the sensor b is divided equally by the straight line h_1, h_2, h_3, and χ, which starting from point$b$, respectively, in this case, the coverage overlap areas of A and B are respectively $S(h_1)$, $S(h_2)$, $S(h_3)$, and $S(\chi)$.

Lemma 4: For an arc length and the radius of the ends forming the perimeter of fan-shaped$A$, when the rotation range of the radiation direction of the sensor b is limited to the left end radius of$A$, as shown in Figure 5 (b), $S(h_2)$ is the minimum coverage overlap area that can be obtained in this case.

Proof: Making a straight line O passing through point b and perpendicular to the left end radius, the shortest distance h_2 from point b to the radius can be used as all the height of the overlapped area formed by the different radiation directions of b within the radius of the left end in Figure 5 (b), and the overlaying areas can be classified into two categories, one is the vertical O which passes the overlapping area, as shown in the example in Figure 6; the other is that the vertical O does not pass the overlapping area, as shown in Figure 7.

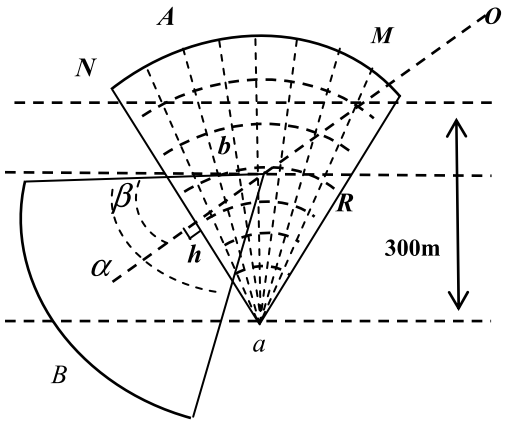

FIGURE 6. The vertical *O* located in radiation zone of sensor *b*.

We assume that there are i kinds of cases where the vertical O passes through the overlapping area, taking Figure 6 as an example, let the vertical O divide the angle α into β and $\alpha-\beta$. The area of any one of the $i-1$ cases covering the overlapped area is:

$$S_{i-1} = \frac{1}{2} \cdot h_2^2 \cdot [\tan\beta + \tan(\alpha - \beta)] \quad (\beta \geq 0 \& \beta \neq \alpha/2)$$

When α is just divided equally by the vertical O, the area of overlay area at this time is $S(h_2)$:

$$S(h_2) = h_2^2 \cdot \tan\frac{\alpha}{2} \tag{22}$$

We assume that there are j kinds of cases in which the vertical O has not been passing through the overlapped area.

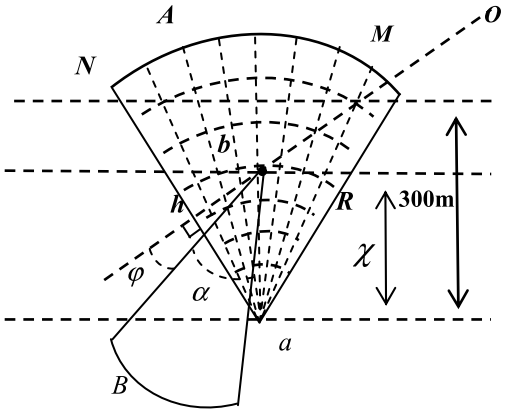

FIGURE 7. The vertical *O* located outside radiation zone of sensor *b*.

Taking Figure 7 as an example, supposing the vertical O and the area B are separated by an angle ϕ, the area covering the overlapping area is:

$$S_j = \frac{1}{2} \cdot h_2^2 \cdot [\tan(\alpha + \varphi) - \tan(\varphi)] \quad (\varphi \geq 0) \tag{23}$$

Since the tangent function is an increasing function in any continuous interval, we can get:

$$2 \cdot \tan\frac{\alpha}{2} < \tan\beta + \tan(\alpha - \beta) \quad (\beta \geq 0 \& \beta \neq \alpha/2) \tag{24}$$

$$2 \cdot \tan\frac{\alpha}{2} < \tan(\alpha + \varphi) - \tan(\varphi) \quad (\varphi \geq 0) \tag{25}$$

It can be proved.

Similarly, we can prove that $S(h_1)$ and $S(h_3)$ are the smallest overlapped areas when the rotation range of the radiation direction of the sensor b is only limited to the upper and right end radius of the A arc length, respectively. Then calculated the overlapping area $S(\chi)$ when the radiation range angle α of sensor b is just split by the straight line χ which starting from the point b. At last, compare the sizes of $S(h_1)$, $S(h_2)$, $S(h_3)$, and $S(\chi)$ to get the smallest overlap area. We assume that the calculated result is $S(h_1) < S(h_2) < S(h_3) < S(\chi)$, $S(h_1)$ is the minimum coverage overlap area. That is, when the overlap ratio is $\eta > \eta_{\text{Threshold}}$, in order to reduce the overlapping coverage as much as possible, the radiation direction of the sensor b is adjusted to the direction when the angle α is just divided by the straight line h_1 starting from the point b.

IV. EXPERIMENTAL SIMULATIONS AND ANALYSIS

A. PERFORMANCE EVALUATION INDEX

1) AVERAGE PACKET LOSS RATE

The average packet loss rate is an important indicator to measure the data transmission efficiency of the vehicular network. The smaller the packet loss rate is, the higher the reliability and effectiveness of the in-vehicle network data transmission[28]. The average packet loss rate γ is defined as:

$$\gamma = 1 - \frac{K_{\text{Packet}}}{M_{\text{Packet}}} \tag{26}$$

TABLE 1. Parameter statistics.

Parameter	Value
Vehicle speed	12m/s~18m/s
Sensor communication radius	400m
Average distance of road sections	1km
Number of vehicles	200~400
Data rate	100kbps
Packet length	2Mbps
Type of service	OmniAnten
MAC protocol	IEEE802.11

M_{Packet} represents the total number of packets sent by the source vehicle, and K_{Packet} represents the total number of packets that the target vehicle has successfully received.

2) TRANSMISSION DELAY

The time delay is a universal problem in the vehicular network, due to the high mobility of vehicle network, the degree of delay is more serious than that of other static networks[29]–[31]. The smaller the time delay, the vehicle network is of higher value in the application. Transmission delay t_{Packet} is defined as the current time at which the target node received the data minus the initial time at which the source node sent data.

3) RECEIVE THE TOTAL AMOUNT OF DATA PACKETS

When the vehicular network carries on the collection of road environment data, the total amount of data packets that the target node finally gets is an important index to evaluate the efficiency of the vehicle network task execution[32], [33]. The total number of received packets P_{total} indicates the number of packets received by all destination nodes after the simulation.

B. EXPERIMENTAL METHODS AND PARAMETERS

In the experimental part, we use the network simulation tool NS-2 to build a simulation scene, the driving data in the experiment process adopts the method of random extraction. For example, in this experiment, we randomly selected the driving data of Xiaogang area and Shayuan area of Guangzhou, China. The road scene has a large traffic volume, a large number of forked sections, and a complex vehicle environment, which has a certain representative value as a test scenario for vehicle network simulation. Vehicle information statistics are as follows:

We use the vehicle trajectory generator VanetMobiSim to simulate the vehicle trajectory. VanetMobiSim is an extension of CanuMobiSim for vehicle mobile application, it can define vehicle trajectory and generate vehicle trajectory trace files needed for VMIT simulation. The final simulation result of the experiment is the average of 100 test results. Among them, the comparison algorithm introduced in this paper is a high mobility vehicle mobile internet of things (LDPR) based on improved path duration proposed by Oliveira [34] and an adaptive vehicle mobile internet of things based on adaptation method (AID) proposed by Bakhouya [35]. And the simulation conditions of all the algorithms are consistent in the experiment. The LDPR algorithm improves the communication duration of the path, reduces the probability of communication interruption, and improves the network communication efficiency by improving the network topology. The AID algorithm uses an adaptive data broadcasting method to reduce data transmission delay, reduce redundant data, and improve communication efficiency. The method of this article is to improve network communication efficiency by covering enhancements and solving the best communication durations. The LDPR algorithm is similar to the research method in this paper, and they all pay attention to the issue of communication duration. And the AID algorithm is different from the method of this paper, but all have the purpose of improving VMIT network communication efficiency. So in the experiment, we use the LDPR algorithm and the AID algorithm to compare with our algorithm respectively, more to highlight the performance advantages of our algorithm.

C. EXPERIMENTAL SIMULATION RESULTS

Figure 8 (a) and (b) shows the average packet loss rate during VMIT simulation under different numbers of vehicles. As can be seen from the figure, as the number of vehicles increases, the average packet loss rate gradually decreases. Combined with data analysis in the figure, the VMIT network has higher communication interruption probability than other networks due to the high-speed mobility and the moving direction of the VMIT network. When the number of vehicles increases, the number of candidate next-hop nodes that can be selected within the communication range of vehicle nodes increases, they can choose to transmit data packets to the nodes closer to them to increase the communication duration, thus reducing the probability of interruption. The probabilistic analysis method adopted by PANM can effectively calculate the relationship between the speed and the communication duration of the source vehicle and the adjacent vehicles so that the source vehicle can select the next-hop node that meets the requirement of the communication duration as much as possible to transmit data and reduce the communication interruption probability. LDPR algorithm adopts the principle of recent communication when the vehicle density is small and adopts the principle of optimal direction when the density is large. Although the current path of the selected next-hop node and the source node is optimal, it lacks the correlation analysis between the speed and the communication duration. Because the variability of the speed of the next-hop node, it cannot guarantee that the communication time can reach the required time for successful data transmission. AID algorithm has no specific analysis of the communication interruption time, and the packet loss rate caused by communication interruption is greater.

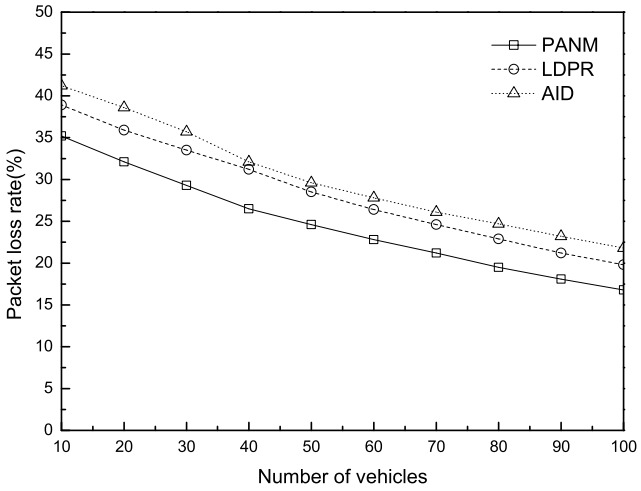

(a) The incremental range of the number of vehicles is 10.

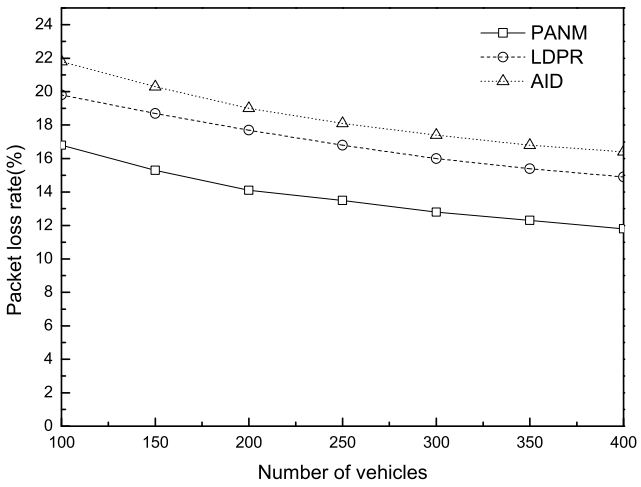

(b) The incremental range of the number of vehicles is 50.

FIGURE 8. Packet loss rate under a number of different vehicles.

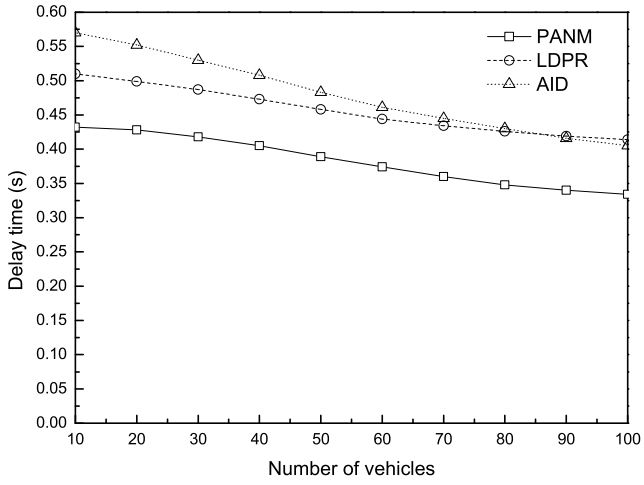

(a) The incremental range of the number of vehicles is 10.

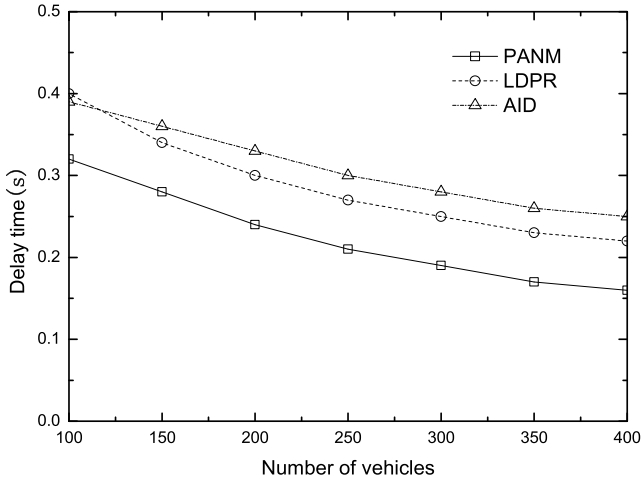

(b) The incremental range of the number of vehicles is 50.

FIGURE 9. Delay time for different number of vehicles.

Figure 9 (a) and (b) shows the data transmission delay under the different number of vehicles. As can be seen from the figure, the delay time gradually decreases as the number of vehicles increases. When the number of vehicles is small, if there are no adjacent vehicles in the communication range of the source node, it needs to travel a certain distance, and data can be forwarded only when there is an adjacent vehicle. In this case, the transmission delay time is relatively large. And when the number of vehicles increases, the number of neighbor nodes in each vehicle node's communication range will increase, thus reducing the time to find neighbor nodes and reducing the delay time. When the vehicle reaches a certain number, each vehicle node at the same time has a neighbor node. At this point, even if the number of vehicles continues to grow, the delay time is no longer affected by the time of finding the neighbor nodes, which mainly depends on the routing strategy adopted by the algorithm. When adopting the routing strategy, the probability of communication interruption is large, the time consumed in data retransmission will increase, and the delay time will also increase, therefore, with the data in the figure, it can be seen that each algorithm is affected by the increasing number of vehicles; the delay time of vehicle communication is reduced. Among them, the PANM algorithm has a better communication persistence mechanism, with fewer delays and fewer retransmissions caused by interrupts.

Figure 10 (a) and (b) shows the total number of data packets received by the target vehicle under different vehicle numbers. After the target node receives the data of the source node during the simulation, it randomly selects the source node and the target node again until the end of the simulation. As can be seen from the figure, PANM algorithm receives more packets in total. This is because the PANM algorithm minimizes the overlapping ratio of the sensing range of the nodes by using the coverage enhancement method while ensuring the communication duration so that more data can be received than the LDPR and AID algorithms.

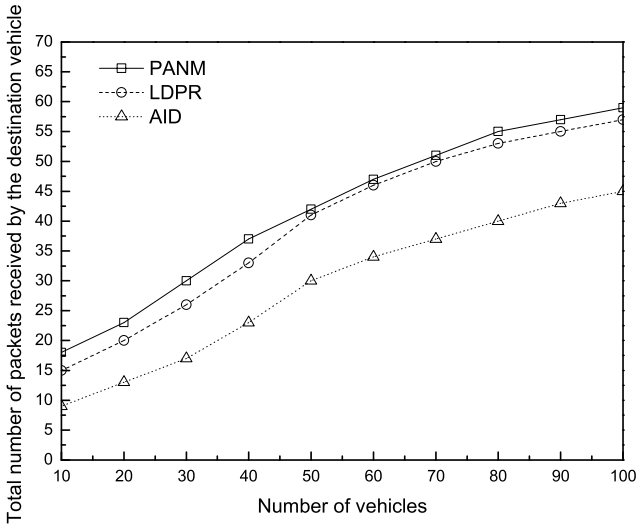

(a) The incremental range of the number of vehicles is 10.

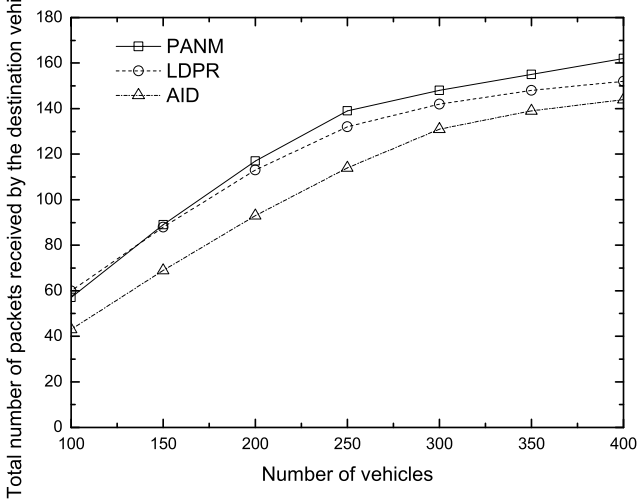

(b) The incremental range of the number of vehicles is 50.

FIGURE 10. The total number of packets received under a number of different vehicles.

V. CONCLUSION

In order to make the vehicle mobile internet of things enhance the network coverage while ensuring the continuity of communication, we propose the PANM algorithm by analyzing the relationship between vehicle speed status, communication duration and network coverage under two common vehicle communication models. The PANM algorithm first analyzes the vehicle spacing distance through a variety of motion conditions between the source vehicle and the target vehicle in communication and obtains the communication duration function. Secondly, under the premise of ensuring the required communication time, we analyze the network coverage of the communication model. We use the method of increasing the distance between the nodes and adjusting the direction of vehicle sensors to improve the network coverage. In the simulation experiment, it can be seen from the comparison of the cases that the PANM algorithm is used or not, respectively, we can see that the PANM has a certain effect in enhancing the coverage of the vehicle mobile internet of things.

REFERENCES

[1] S. K. Datta, R. P. F. Da Costa, J. Harri, and C. Bonnet, "Integrating connected vehicles in Internet of Things ecosystems: Challenges and solutions," presented at the IEEE 17th Int. Symp. World Wireless, Mobile Multimedia Netw., Coimbra, Portugal, Jun. 2016.

[2] D. Kombate and L. N. Wang, "The Internet of vehicles based on 5G communications," in *Proc. IEEE Int. Conf. Internet Things*, Chengdu, China, Dec. 2016, pp. 445–448.

[3] R. Hajlaoui, H. Guyennet, and T. Moulahi, "A survey on heuristic-based routing methods in vehicular ad-hoc network: Technical challenges and future trends," *IEEE Sensors J.*, vol. 16, no. 17, pp. 6782–6792, Sep. 2016.

[4] W.-H. Lee, K.-P. Hwang, and W.-B. Wu, "An intersection-to-intersection travel time estimation and route suggestion approach using vehicular ad-hoc network," *Ad Hoc Netw.*, vol. 43, pp. 71–81, Jun. 2016.

[5] O. Kaiwartya, A. H. Abdullah, Y. Cao, A. Altameem, M. Prasad, C.-T. Lin, and X. Liu, "Internet of vehicles: Motivation, layered architecture, network model, challenges, and future aspects," *IEEE Access*, vol. 4, pp. 5356–5373, 2016.

[6] X. Hu, K. Wang, X. Liu, Y. Sun, P. Li, and S. Guo, "Energy management for EV charging in software-defined green vehicle-to-grid network," *IEEE Commun. Mag.*, vol. 56, no. 5, pp. 156–163, May 2018.

[7] L. Du and H. Dao, "Information dissemination delay in vehicle-to-vehicle communication networks in a traffic stream," *IEEE Trans. Intell. Transp. Syst.*, vol. 16, no. 1, pp. 66–80, Feb. 2015.

[8] R. C. Daniels and R. W. Heath, Jr., "Link adaptation with position/motion information in vehicle-to-vehicle networks," *IEEE Trans. Wireless Commun.*, vol. 11, no. 2, pp. 505–509, Feb. 2012.

[9] N. Kumar, N. Chilamkurti, and J. H. Park, "ALCA: Agent learning—Based clustering algorithm in vehicular ad hoc networks," *Pers. Ubiquitous Comput.*, vol. 17, no. 8, pp. 1683–1692, 2013.

[10] S. Ucar, S. C. Ergen, and O. Ozkasap, "VMaSC: Vehicular multi-hop algorithm for stable clustering in Vehicular Ad Hoc Networks," in *Proc. IEEE Wireless Commun. Netw. Conf.*, Apr. 2013, pp. 2381–2386.

[11] C. Campolo, A. Molinaro, A. Iera, and F. Menichella, "5G network slicing for vehicle-to-everything services," *IEEE Wireless Commun.*, vol. 24, no. 6, pp. 38–45, Dec. 2017.

[12] S. Chen, J. Yang, Y. Li, and J. Yang, "Multiconstrained network intensive vehicle routing adaptive ant colony algorithm in the context of neural network analysis," *Complexity*, vol. 2017, Sep. 2017, Art. no. 8594792.

[13] E. Ndashimye, S. K. Ray, N. I. Sarkar, and J. A. Gutiérrez, "Vehicle-to-infrastructure communication over multi-tier heterogeneous networks: A survey," *Comput. Netw.*, vol. 112, pp. 144–166, Jan. 2017.

[14] T. Suzuki and T. Fujii, "Joint routing and spectrum allocation for multi-hop inter-vehicle communication in cognitive radio networks," *Int. J. Intell. Transp. Syst. Res.*, vol. 15, no. 1, pp. 39–49, 2017.

[15] L. Jin, G. Zhang, and J. Wang, "Probabilistic model checking-based survivability analysis in vehicle-to-vehicle networks," *China Commun.*, vol. 15, no. 1, pp. 118–127, Jan. 2018.

[16] W. Huang, L. Ding, D. Meng, J.-N. Hwang, Y. Xu, and W. Zhang, "QoE-based resource allocation for heterogeneous multi-radio communication in software-defined vehicle networks," *IEEE Access*, vol. 6, pp. 3387–3399, 2018.

[17] T. Rattanamanee, S. Nanthavanij, and V. Ammarapala, "Vehicle dispatching for minimizing arrival conflicts in multi-supplier logistics network," *Arabian J. Sci. Eng.*, vol. 43, no. 6, pp. 3187–3198, 2018.

[18] F. Liu, Z. Chen, and B. Xia, "Data dissemination with network coding in two-way vehicle-to-vehicle networks," *IEEE Trans. Veh. Technol.*, vol. 65, no. 4, pp. 2445–2456, Apr. 2016.

[19] J. Zhu and B. Wang, "The optimal placement pattern for confident information coverage in wireless sensor networks," *IEEE Trans. Mobile Comput.*, vol. 15, no. 4, pp. 1022–1032, Apr. 2016.

[20] B. Wang, J. Zhu, L. T. Yang, and Y. Mo, "Sensor density for confident information coverage in randomly deployed sensor networks," *IEEE Trans. Wireless Commun.*, vol. 15, no. 5, pp. 3238–3250, May 2016.

[21] J. Wang, K. Liu, K. Xiao, C. Chen, W. Wu, V. C. Lee, and S. H. Son, "Dynamic clustering and cooperative scheduling for vehicle-to-vehicle communication in bidirectional road scenarios," *IEEE Trans. Intell. Transp. Syst.*, vol. 19, no. 6, pp. 1913–1924, Jun. 2018.
[22] P. Thulasiraman, G. A. Clark, and T. M. Beach, "Applying location estimation for reliable routing in tactical unmanned ground vehicle networks," *Peer-Peer Netw. Appl.*, vol. 10, no. 4, pp. 1034–1050, 2017.
[23] A. S. H. Mahmoud and A. H. Rashed, "Efficient computation of distribution function for sum of large number of lognormal random variables," *Arabian J. Sci. Eng.*, vol. 39, no. 5, pp. 3953–3961, 2014.
[24] S. J. Fletcher and A. S. Jones, "Multiplicative and additive incremental variational data assimilation for mixed lognormal–Gaussian errors," *Monthly Weather Rev.*, vol. 142, no. 7, pp. 2521–2544, 2014.
[25] L. Wei, H. Zhang, Z.-Q. Wei, and T. A. Gulliver, "Performance analysis of mobile vehicle-to-vehicle communication in n-Rayleigh fading channels," *Yingyong Kexue Xuebao/J. Appl. Sci.*, vol. 33, no. 4, pp. 367–375, 2015.
[26] X. Li, J. Liu, Q. Yao, and J. Ma, "Efficient and consistent key extraction based on received signal strength for vehicular ad hoc networks," *IEEE Access*, vol. 5, no. 99, pp. 5281–5291, 2017.
[27] N. Cheng, H. Zhou, L. Lei, N. Zhang, Y. Zhou, X. Shen, and F. Bai, "Performance analysis of vehicular device-to-device underlay communication," *IEEE Trans. Veh. Technol.*, vol. 66, no. 6, pp. 5409–5421, Jun. 2017.
[28] W. Nie, V. C. S. Lee, D. Niyato, Y. Duan, K. Liu, and S. Nutanong, "A quality-oriented data collection scheme in vehicular sensor networks," *IEEE Trans. Veh. Technol.*, vol. 67, no. 7, pp. 5570–5584, Jul. 2018.
[29] S. Caixing and Z. Jianhua, "Research of the multi-way connectivity probability for platoon-based vehicle-to-infrastructure communication network," *J. China Universities Posts Telecommun.*, vol. 23, no. 1, pp. 1–7, 2016.
[30] W. Wei, M. Woźniak, R. Damaševičius, X. Fan, and Y. Li, "Algorithm research of known-plaintext attack on double random phase mask based on WSNs," *J. Internet Technol.*, vol. 20, no. 1, pp. 39–48, 2019.
[31] W. Wei, J. Su, H. Song, H. Wang, and X. Fan, "CDMA-based anti-collision algorithm for EPC global C1 Gen2 systems," *Telecommun. Syst.*, vol. 67, no. 1, pp. 63–71, Jan. 2019.
[32] J.-P. Gehrmann and G. Sporer, "Higher bandwidth automotive-grade Ethernet and distributed vehicle networks," *ATZelektronik Worldwide*, vol. 11, no. 6, pp. 60–65, 2016.
[33] J. Ruan, Y. Wang, F. T. S. Chan, X. Hu, M. Zhao, F. Zhu, B. Shi, Y. Shi, and F. Lin, "A life cycle framework of green IoT-based agriculture and its finance, operation, and management issues," *IEEE Commun. Mag.*, vol. 57, no. 3, pp. 90–96, Mar. 2019.
[34] R. Oliveira, M. Luís, A. Furtado, R. Dinis, and P. Pinto, "Improving path duration in high mobility Vehicular Ad Hoc Networks," *Ad Hoc Netw.*, vol. 11, no. 1, pp. 89–103, 2013.
[35] M. Bakhouya, J. Gaber, and P. Lorenz, "An adaptive approach for information dissemination in Vehicular Ad hoc Networks," *J. Netw. Comput. Appl.*, vol. 34, no. 6, pp. 1971–1978, Nov. 2011.

ZHIPING WAN was born in Hubei, China, in 1980. He received the bachelor's degree from Huanggang Normal College, in 2003, and the master's degree from the Guangdong University of Technology, in 2008. He was a Teacher with the Huali College of Guangdong University of Technology from 2004 to 2008. Since 2010, he has been an Associate Professor with the Department of Information Science, Xinhua College of Sun Yat-sen University, where he recently became a Visiting Scholar. He has published 59 papers and holds two patents and one invention. His research interests include wireless sensor networks, cognitive radio networks, and network security.

ZHIHONG PAN was born in Guangdong, China, in 1984. He received the B.Eng. degree from the Dongguan University of Technology, Dongguan, China, in 2008, and the M.Eng. degree from Jinan University, Guangzhou, China, in 2011. He has been a Senior Engineer with the Department of Information Science, Xinhua College of Sun Yat-sen University, since 2015. He has published 14 papers and holds three patents. His research interests include the Internet of Things, crowdsourcing, and machine learning.

WEICHUAN NI was born in Guangdong, China, in 1990. He received the bachelor's degree from the Xinhua College of Sun Yat-sen University, in 2014, where he is currently a Lab Manager with the Equipment and Laboratory Management Department. He has published six papers and holds one patent and one invention. His research interests include machine vision and wireless sensor networks.

FENG WANG was born in Hebei, China, in 1984. She graduated from Hebei Polytechnic University, in 2006, and received the master's degree from Jinan University, in 2008. Since 2008, she has been a Lecturer with the Department of Information Science, Xinhua College of Sun Yat-sen University. She has published 29 papers, holds two patents and one invention. Her research interests include signal and information processing and automation technology.

ZEMIN QIU was born in Guangdong, China, in 1983. She received the bachelor's degree from the Guangdong University of Technology, in 2007, and the master's degree from Sun Yat-sen University, in 2011. Since 2013, she has been a Lecturer with the Department of Information Science, Xinhua College of Sun Yat-sen University. She has published seven papers and holds one patent. Her research interests include machine learning and intelligent algorithms.

SHAOJIANG LIU was born in Guangdong, China, in 1991. He received the bachelor's degree from the Xinhua College of Sun Yat-sen University, in 2014, and the master's degree from the South China University of Technology, in 2019. He is currently an Experimental Technical Personnel with the Xinhua College of Sun Yat-sen University. He has published ten papers and holds two patents and one invention. His research interests include wireless networks and machine learning.

ZHIMING XU was born in Guangdong, China, in 1996. He received the bachelor's degree from the Xinhua College of Sun Yat-sen University, in 2019, where he is currently a Lab Manager with the School of Information Science. He holds three patents and two inventions. His research interests include embedded systems and wireless sensor networks.